Molecular Crystals and Liquid Crystals Science and Technology. Section A. Molecular Crystals and Liquid Crystals

Publication details, including instructions for authors and subscription information:
http://www.tandfonline.com/loi/gmcl19

Transitions to Ordered Phases in Systems Containing Rod-like Particles: II. Continuum Monte Carlo Approach versus Discrete Lattice Models

Larry A. Chick [a] & Christopher Viney [b]

[a] Pacific Northwest Laboratory, Richland, WA, 99352

[b] Center for Bioengineering, University of Washington, Seattle, WA, 98195

Version of record first published: 24 Sep 2006.

To cite this article: Larry A. Chick & Christopher Viney (1993): Transitions to Ordered Phases in Systems Containing Rod-like Particles: II. Continuum Monte Carlo Approach versus Discrete Lattice Models, Molecular Crystals and Liquid Crystals Science and Technology. Section A. Molecular Crystals and Liquid Crystals, 226:1, 41-61

To link to this article: http://dx.doi.org/10.1080/10587259308028790

Mol. Cryst. Liq. Cryst., 1993, Vol. 226, pp. 41–61
Reprints available directly from the publisher
Photocopying permitted by license only

Printed in the United States of America

Transitions to Ordered Phases in Systems Containing Rod-like Particles: II. Continuum Monte Carlo Approach versus Discrete Lattice Models

LARRY A. CHICK

Pacific Northwest Laboratory, Richland, WA 99352

and

CHRISTOPHER VINEY

Center for Bioengineering, University of Washington, Seattle, WA 98195

(Received October 31,1991; in final form July 24, 1992)

The predictions of the new continuous-placement Monte Carlo (CMC) approach described in the preceding paper are compared with the results obtained from the discrete lattice model (DLM) of Flory and Ronca. The comparison is made for two-dimensional, monodisperse, athermal systems. For this purpose, we have adapted the Flory-Ronca model to two dimensions, gaining additional insight into the justification for one of the numerical correction factors used in that model. The CMC and DLM approaches both predict that a uniform (flat) distribution of rod orientations in the anisotropic phase is associated with a first-order isotropic-to-nematic transition, while normally distributed orientations lead to a continuous transition with increasing rod concentration. The two models also agree qualitatively with respect to the relative free energies of different rod orientation distributions in the anisotropic phase. However, the DLM assigns disproportionately high entropy to short rods (especially at high concentrations) and to disordered phases, so that the DLM does not generate quantitatively reliable phase diagrams.

Keywords: lattice model, Monte Carlo, nematic, phase separation, rod-like particles, two-dimensional

INTRODUCTION

In the preceding paper,[1] we described a continuous Monte Carlo (CMC) method for measuring the combinatoric entropy, S_c, in systems of rigid rod-like particles. The method was employed for a two-dimensional system of monodisperse, athermal rods. Phase equilibria were predicted for systems with imposed long-range order, for which the orientational entropy, S_o, can be calculated exactly. Separation of isotropic and anisotropic phases is predicted for systems in which uniform distributions of rod orientations are imposed on the anisotropic phase. On the other

hand, phase evolution—the smooth increase of orientational order as the rod concentration is increased—is predicted for systems with normally distributed rod orientations imposed.

In the CMC method, rod positions and orientations are allowed to vary continuously, unlike the segmented rods in Flory's[2,3] discrete lattice model (DLM), wherein the rod segments are restricted to lattice cells having long-range positional order. In the present paper, the results of the DLM are compared to those of the CMC. These comparisons demonstrate that the DLM assigns unduly high entropy to shorter rods relative to longer rods; in a thermodynamic sense the DLM "favors" shorter rods. To a lesser extent, the DLM thermodynamically favors disorder relative to order in monodisperse systems. However, the DLM is found to be a good predictor of orientational distribution shape in monodisperse systems. In the following paper[4] four fundamental causes of the DLM's predictive errors are discussed.

Unlike Flory,[2,3] we calculate the orientational entropy, S_o, independently of the discrete lattice. As discussed in the preceding paper,[1] S_o is calculated exactly, based on the imposed orientational distribution. The DLM and CMC methods used in the present work differ only in their techniques for determining the vacancy fractions, ν_j, used in calculating the combinatoric entropy, S_c (see Equation 7 in the preceding paper[1]). Once S_c and S_o are determined, the techniques of establishing phase equilibria covered in the preceding paper[1] are identical for both the CMC and the DLM.

Flory's Computation of Vacancy Fractions

Finding a tractable way to predict the combinatoric entropy is the real challenge for models dealing with liquid crystals, because the number of ways to position a rod within the system is a function of both the orientation of the rod being placed and the distribution of orientations of the rods already present in the configuration. Flory[2] solved this problem brilliantly by using a discrete lattice model. It is useful to re-trace Flory's published development of the DLM, using a somewhat more transparent approach with additional, intermediate steps. The following treatment will a) refresh the reader's memory with regard to the original Flory model,[2] b) explain a $4/\pi$ correction factor that was subsequently inserted by Flory and Ronca,[3] and c) serve as a prelude to the development of our improved, high resolution lattice model, that is discussed in the following paper.[4]

In Flory's model the domain axis is one of the principal axes of the lattice. A rod that is oriented at an angle, ψ, from the preferred domain axis is represented as a stair-step arrangement of sequences of occupied cells, each of which runs parallel to the preferred domain axis (see Figure 1 in Flory and Ronca[3]). Each rod is the width of one lattice cell and is represented by x occupied cells; thus x is the axial ratio. The total number of cells within the entire lattice is n_0, n_1 is the number of vacant cells (or cells occupied by solvent), and n_x is the number of rods. Then the rod concentration, or volume fraction, V_x is given by:

$$V_x = \frac{xn_x}{n_0} = \frac{xn_x}{n_1 + xn_x} \tag{1}$$

The problem is to express the number of situations, or appropriate vacancies, $\nu_{(j+1)}$, that are available to the $(j + 1)^{th}$ rod once j rods have already been placed in the matrix. The $(j + 1)^{th}$ rod has a particular disorientation from the preferred domain axis, ψ, which is represented by its particular number of sequences, y, also referred to as its disorientation index. Since the angle of the rod is predetermined, the series of cells within the lattice that must be found to be vacant in order to accommodate the rod is uniquely determined by selecting the position to be occupied by the very first cell of the rod. Then the probability of successfully placing the $(j + 1)^{th}$ rod by randomly selecting a position for its first cell is given by:

$$\frac{\nu_{j+1}}{n_0} = \text{Probability of placement} \tag{2}$$

Also, since the rod is composed of y sequences, the probability of placing the rod becomes the product of the probabilities of successfully placing each sequence:

$$\frac{\nu_{j+1}}{n_0} = (P_{\text{seq }1})(P_{\text{seq }2}) \cdots (P_{\text{seq }y}) \tag{3}$$

The problem reduces to that of finding the placement probability for a sequence. (One of Flory's assumptions is that the probability for each sequence is the same.) Each sequence is considered to be composed of a first cell and the required number of remaining cells. The probability of finding a vacancy for the first cell is given simply by the fraction of vacant cells in the matrix:

$$(P_{\text{first cell}}) = \frac{n_1}{n_0} \tag{4}$$

Once the first cell of the sequence has been placed successfully, there are only two types of cells that can compete for the next space in line, vacancies and first cells of sequences that have already been placed. Because the sequences are arranged parallel to the domain axis, the fact that the first cell has been placed guarantees that only the first cell of an existing sequence can block placement of the next cell in the sequence being placed. It is apparent that the same situation holds for all of the remaining cells in the sequence being placed, as long as they are placed sequentially, so we have:

$$(P_{\text{remaining cell}}) = \left(\frac{n_1}{n_1 + \sum_{i=1}^{n_s} y_i} \right) \tag{5}$$

where the summation in the denominator expresses the total number of first cells of sequences already existing in the lattice. Combining (4) and (5) and accounting

for the fact that there are $(x/y) - 1$ remaining cells in a sequence, we have for the probability of placing a sequence:

$$(P_{\text{seq}}) = \left(\frac{n_1}{n_0}\right)\left(\frac{n_1}{n_1 + \sum_{i=1}^{n_x} y_i}\right)^{(x/y-1)} \tag{6}$$

Since there are y such sequences, the fraction of appropriate vacancies for the entire rod becomes:

$$\frac{\nu_{j+1}}{n_0} = \left[\left(\frac{n_1}{n_0}\right)\left(\frac{n_1}{n_1 + \sum_{i=1}^{n_x} y_i}\right)^{(x/y-1)}\right]^{(y)} \tag{7}$$

which reduces to:

$$\frac{\nu_{j+1}}{n_0} = \left(\frac{n_1}{n_0}\right)^{y}\left(\frac{n_1}{n_1 + \sum_{i=1}^{n_x} y_i}\right)^{(x-y)} \tag{8}$$

This elegantly simple expression is the key to Flory's model. (We shall see later, however, that this expression introduces some problems.) The first factor in (8) accounts for placement of the first cells of the y sequences and the second factor accounts for the x-y remaining cells. It is the construction of the rods within the lattice, with parallel sequences—the number of which depends on the disorientation of the rod—that allows the partitioning of the rod placement probability into these two simple factors.

Flory next incorporated a mean field, or average representation of the degree of disorder in the system, $\hat{y}$, which is the average of the number of sequences required to represent rods in the lattice, given a particular distribution of disorientations, and is defined by:

$$\hat{y} = \frac{1}{n_x}\sum_{i=1}^{n_x} y_i \tag{9}$$

(We shall see later that use of the mean field concept also introduces inaccuracies into the DLM.) Using only very conservative approximations[3] and converting to volume fractions through (1) we obtain:

$$\frac{\nu_j}{n_0} = \left[\frac{1 - V_x}{1 - V_x(1 - \hat{y}/x)}\right]^{(x)}\left[1 - V_x\left(1 - \frac{\hat{y}}{x}\right)\right]^{(y_j)} \tag{10}$$

where the subscript, j, has been written on the exponent of the second factor to emphasize that this is the disorder index for the rod being placed, while $\hat{y}$ represents the average disorder of the configuration.

Conversion to Two Dimensions

Conversion of Flory's model to two dimensions does not affect Equations (1) through (10); we simply substitute A_f, the area fraction occupied by rods, for the volume fraction, V_x, in (1) and (10). However, the appropriate expressions for y and $\hat{y}$ in the square lattice are different from those used by Flory and Ronca[3] in the cubic lattice. The conversion leads to a problem involving the proper calculation of vacancy fractions in the two-dimensional isotropic phase.

In the cubic lattice model, Flory and Ronca used:

$$y = \frac{4}{\pi} x \sin \psi \tag{11}$$

to express the number of sequences necessary to represent a rod with polar angular deviation from the preferred domain axis, ψ. The preferred domain axis is chosen as one of the principal axes of the cubic lattice. The $4/\pi$ factor in (11) was justified by Flory and Ronca to account for averaging over the angle of rotation about the domain axis, ϕ. All rods with polar angle, ψ, are thermodynamically equivalent, regardless of their rotational angle, ϕ. However, rods having ϕ values such that they are not parallel to one of the remaining two principal lattice axes will require representation by extra sequences to account for their running more or less diagonally between the principal lattice planes.

Flory and Ronca's expression for the number of sequences, (11), is problematic because it overestimates the number of sequences for rods having high angular disorientation (a rod with $\psi = \pi/2$ is assigned $4x/\pi$ sequences, even though it cannot be composed of more sequences than cells) and underestimates y for rods with perfect or nearly perfect alignment (a rod with perfect alignment is assigned zero sequences, even though it must be composed of exactly one sequence). However, inclusion of the $4/\pi$ factor is convenient because it results in the average number of sequences, $\hat{y}$, for the isotropic phase being equal to the axial ratio, x. For any distribution, $\hat{y}$ is given by (see 11).

$$\hat{y} = \frac{4}{\pi} x \langle \sin \psi \rangle \tag{12}$$

where $\langle \sin \psi \rangle$ is averaged over the distribution. For the three-dimensional isotropic phase, we have:

$$\langle \sin \psi \rangle_{\text{iso,3-D}} = \frac{\pi}{4} \tag{13}$$

which, when substituted into (12) gives:

$$\hat{y}_{\text{iso,3-D}} = x \tag{14}$$

The importance of this result is understood by referring to Equation (10). When the fraction-of-vacancies is calculated for the three-dimensional isotropic phase, $\hat{y} = x$ results in the second factor and the denominator of the first factor in (10) being unity, and the expression reduces to:

$$\left(\frac{\nu_j}{n_0}\right)_{\text{iso,3-D}} = (1 - V_x)^{(x)} \tag{15}$$

We see that the number of vacancies for a rod in the isotropic phase is dependent only upon the rod concentration and the axial ratio, *not on the orientation of the particular rod*. This is proper since, in the isotropic phase, all rod orientations must be equivalent. Although it is never explained clearly in any of Flory's publications, the necessity that all rods be equivalent in the isotropic phase certainly appears to be the major justification for adopting Equation (11). Note that, because of this result, the presupposition of a preferred domain axis has no effect on the calculation of the number of vacancies for the isotropic phase; all reference to angular disorientation from the preferred domain axis is removed from Equation (15). Furthermore, because reference to y is removed from calculations for the isotropic phase, the overestimation of y for rods with high disorientation becomes moot. (It is interesting to note also that the inclusion of the $4/\pi$ factor in Flory and Ronca's 1979[3] version of the model appears to have been motivated by Straley's criticisms in his 1973 paper[5]).

In the case of the two-dimensional system, we cannot justify inclusion of the $4/\pi$ factor in the expression for the number of sequences, since all rods lie in the plane of both principal axes. Instead, we must use:

$$y_{2\text{-D}} = x \sin \psi \tag{16}$$

which leads to:

$$\hat{y}_{\text{iso,2-D}} = \frac{2x}{\pi} \tag{17}$$

Unfortunately, therefore, use of (10) for the two-dimensional isotropic phase will result in dependence of the number of available vacancies on the disorientation of the rod being placed. Hence, although Flory's fundamental equation for the number of available vacancies is conceptually valid in two dimensions, it becomes invalid when coupled with an appropriate expression for the average number of segments. This problem becomes moot when dealing with anisotropic phases having normally distributed orientations because these lead to the prediction of a continuous phase transition, with the isotropic phase never appearing. For phases having uniform orientation distributions, it is instructive to calculate phase diagrams, treating the isotropic phase as a limiting case of the anisotropic phase, wherein the maximum allowable disorientation, ψ^+, is set to $\pi/2$.

For all two-dimensional configurations, we calculate the DLM-based vacancy fractions by averaging over the distribution, because at any given concentration

we want v_j/n_0 to express the average probability of placing a rod when that rod is chosen at random from the global orientation distribution. Therefore, we use:

$$\left(\frac{v_j}{n_0}\right)_{2\text{-D}} = \left[\frac{1 - A_f}{1 - A_f(1 - \hat{y}/x)}\right]^{(x)} \int_{\psi=0}^{\psi=\pi/2} m_\psi[1 - A_f(1 - \hat{y}/x)]^{(x \sin \psi)}\, d\psi \quad (18)$$

where A_f is the rod concentration in two dimensions, and m_ψ is the proportion of rods in the particular distribution with disorientation, ψ.

Alternative Expression for the Number of Sequences

In addition to using (16), we have performed DLM calculations using:

$$y = 1 + (x - 1)\sin \psi \quad (19)$$

This is the two-dimensional analog of the expression proposed by Warner[6]; see also Romanko and Carr[7] for a discussion of variations on the number-of-sequences expression. Equation (19) overcomes one of the problems encountered with (16), in that (19) correctly assigns one sequence to perfectly aligned rods. This becomes important in calculations for phases with nearly perfect order. Calculation of vacancy fractions using (19) requires substitution of $1 + (x - 1)\sin \psi$ for $x \sin \psi$ in the exponent of the integrand in (18).

RESULTS

Comparison of Vacancy Fractions

The fraction-of-vacancies obtained from the DLM, v_j/n_0, is the ratio of the number of ways available for placing the j^{th} rod successfully to the total number of ways originally available for placing rods of a given orientation in the empty system. In the DLM we have a definite count of the number of ways originally available for placing rods in the system; it is simply n_0, the total number of discrete lattice cells. However, as discussed in the preceding paper,[1] in the CMC algorithm, rod position varies continuously, or at least in such small increments for the variation to be essentially continuous. Thus, for treatment of the CMC data, we express the fraction of occupiable vacancies as v_j/K, where K is some very large, unknown number (referenced to the empty system). Therefore, in comparing the CMC results to those of the DLM, we compare vacancy *fractions* (v_j/n_0 to v_j/K), not numbers of vacancies. When we wish to compare the free energy curves, we put the CMC results on the same basis as the DLM results by setting K equal to the equivalent n_0 value, which is the area of the placement square in rod lengths squared multiplied by the square of the axial ratio.[8]

Figure 1 compares log vacancy fraction curves for isotropic distributions at three axial ratios. The solid curves are from polynomials fit to the CMC data. The DLM results (dotted curves) indicate increasing overestimation of vacancy fractions as the axial ratio is decreased. The results for $x = 100$ are in close agreement, with

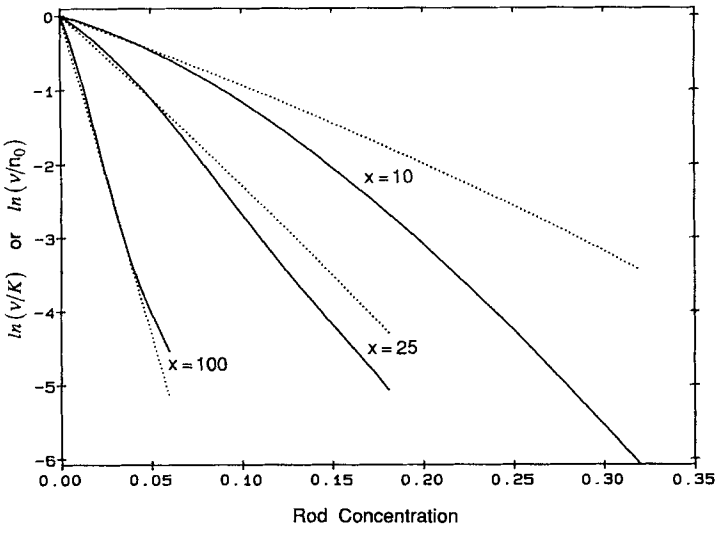

FIGURE 1 Fraction-of-vacancies curves for various axial ratios. All configurations are isotropic. Dotted curves are for the DLM with $y = 1 + (x - 1)\sin\psi$. Solid curves are for CMC data.

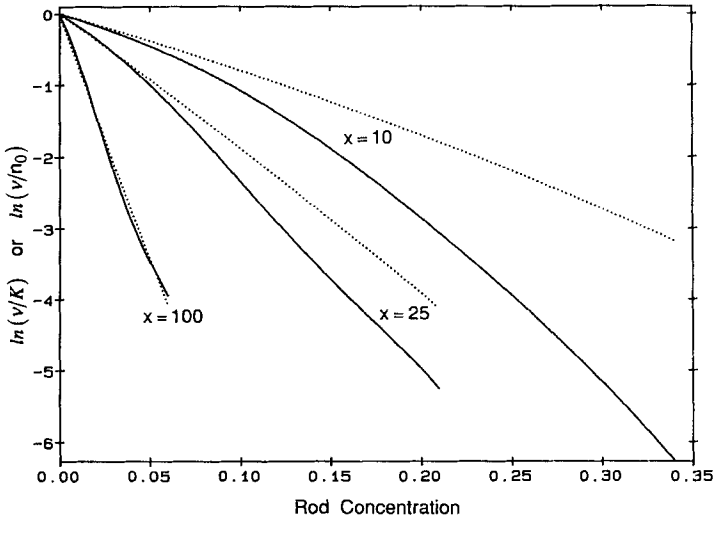

FIGURE 2 Fraction-of-vacancies curves for various axial ratios. All configurations have normally distributed orientations with $\sigma = 40°$. Dotted curves are for the DLM with $y = 1 + (x - 1)\sin\psi$. Solid curves are for CMC data.

an inflection in the CMC curve indicating that the DLM underestimates the vacancy fractions at high concentrations for these long rods. Figure 2 shows similar results at the same three axial ratios when the orientations are normally distributed with σ, the standard deviation of the distributions, set to 40°. These distributions are wide, having an effective degree of disorder near to that of the isotropic phase.

In Figure 3 we see that, for long rods ($x = 100$), the two methods are in close

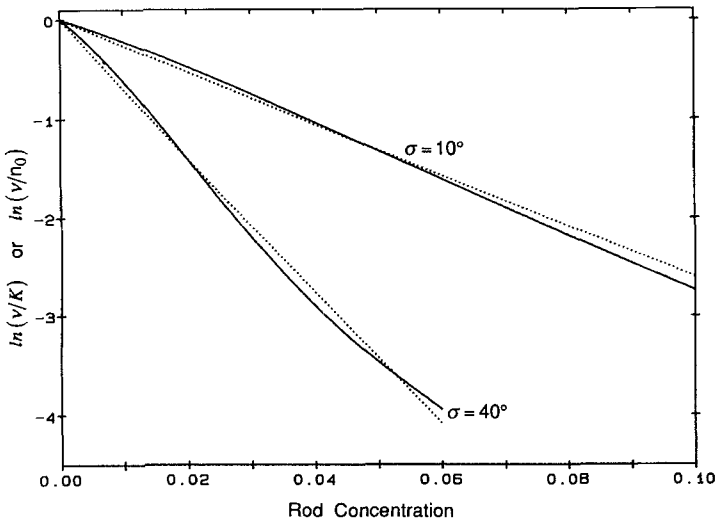

FIGURE 3 Fraction-of-vacancies curves for configurations that have normally distributed orientations with $\sigma = 10°$ or 40°. Axial ratio is 100. Dotted curves are for the DLM with $y = 1 + (x - 1)\sin\psi$. Solid curves are for CMC data. Note that the axes are expanded in scale relative to Figure 2.

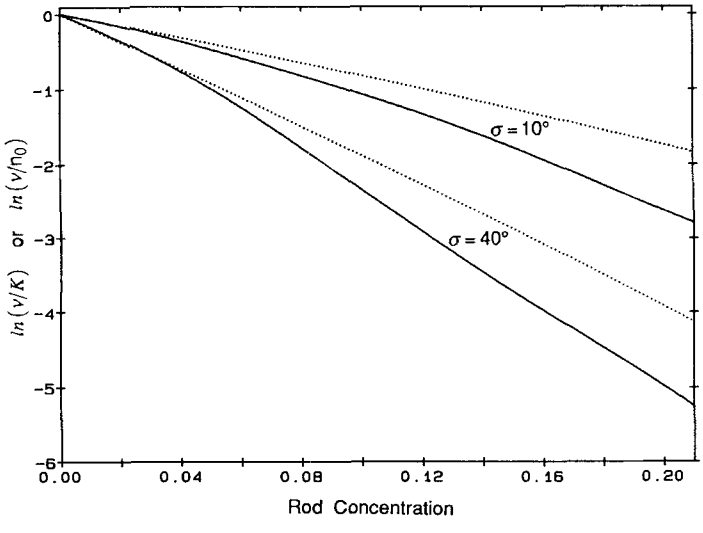

FIGURE 4 Fraction-of-vacancies curves for configurations that have normally distributed orientations with $\sigma = 10°$ or 40°. Axial ratio is 25. Dotted curves are for the DLM with $y = 1 + (x - 1)\sin\psi$. Solid curves are for CMC data.

agreement for both a wide ($\sigma = 40°$) distribution and a relatively narrow ($\sigma = 10°$) distribution. Similarly, the indicated overestimation of vacancy fractions by the DLM is relatively unaffected by the width of the distribution for shorter rods ($x = 25$), as shown in Figure 4. In all of these figures, we used Equation (19) for the DLM calculations, since it provides a more reasonable representation of the number of required sequences for rods with small disorientation.

In general, these results show that the DLM tends to "favor" short rods relative to long rods; that is, the DLM assigns relatively higher vacancy fractions to short rods than to long rods. This discrepancy apparently increases with increasing rod concentration. Although this could be expected to cause serious distortions to DLM treatment of *polydisperse* systems[9-14] it is insignificant in the determination of phase equilibria in monodisperse systems, where all that matters is the relative positions and slopes of the free energy curves for phases having the same axial ratios. We shall see in the next two sections that the errors introduced by the DLM in determination of monodisperse phase equilibria are relatively minor compared to the indicated problems (Figures 1 and 2) for polydisperse systems.

Phase Equilibria for Uniform Orientation Distributions

The differences between the CMC results for monodisperse systems and those of the DLM are relatively minor, as can be seen in the comparison of free energy curves in Figure 5. All curves are for $x = 40$; those specifically pertaining to the anisotropic phase were calculated for $\langle\psi\rangle = 15°$. Pairs of curves from three different calculation methods are shown; the following observations will become more apparent when we discuss the expanded views that are shown in Figures 7 and 8:

a) For both the anisotropic and the isotropic phases, the CMC curves have the highest free energies of the three calculation methods.

b) DLM results using $y = x \sin\psi$ have the lowest free energies for both phases. These results will be referred to as "DL0".

c) DLM results using $y = 1 + (x - 1)\sin\psi$ produced the curves with intermediate free energies. These will be abbreviated "DL1".

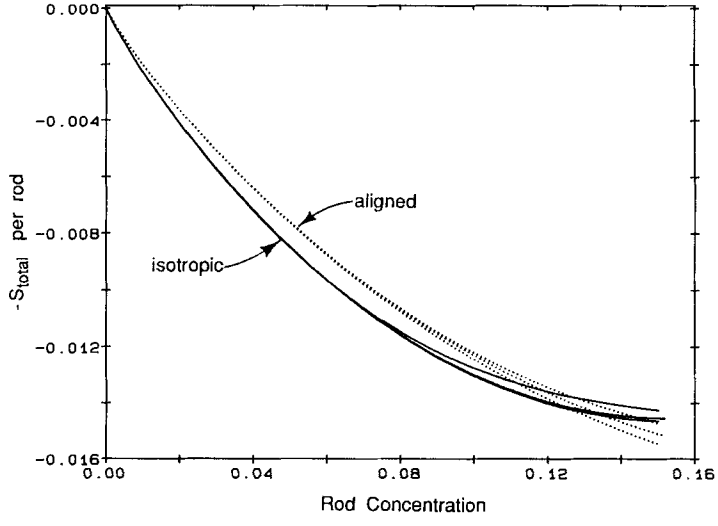

FIGURE 5 Free energy curves for axial ratio of 40. Solid lines are for the isotropic phase, dotted lines are for anisotropic configurations with uniform orientation distributions imposed, $\langle\psi\rangle = 15°$. For each line type, the upper curve is generated by the CMC method, the lower curve is for the DLM with $y = x \sin\psi$, the middle curve is for the DLM with $y = 1 + (x - 1)\sin\psi$. See Figures 7 and 8 for expanded views of the behavior at high rod concentrations.

We will look at these sets of curves in more detail after describing the results on the (partial) phase diagram shown in Figure 6. Phase boundaries for DL0 are the solid lines, those for DL1 are dotted. CMC results, discussed previously (see Figure 8 in the preceding paper[1]), were obtained at three axial ratios, 100, 40, and 25, and they are shown as circles for the lower phase boundary and triangles for the upper phase boundary. The CMC results for the lower phase boundary agree closely with those of DL0, but appear at slightly lower concentrations than those of DL1 at the smaller axial ratios. The CMC results for the upper phase boundary are at noticeably lower concentrations than those of either DL model.

Let us now return to the sets of free energy curves to ascertain how they have resulted in the different phase boundaries: Figure 7 is detail from Figure 5 in the region of the common tangents, which are included on this plot. Only the CMC and DL0 curves are shown, with the curves for the isotropic phase labeled "MCI" and "DL0I" and those for the anisotropic phase marked "MCA" and "DL0A". Notice three features:

a) MCI and DL0I are separated by roughly the same increment of free energy as are MCA and DL0A.

b) MCI and DL0I are nearly parallel, especially so near the left side, where they meet their respective common tangents.

c) The slope of DL0A is slightly greater than that of MCA.

The cumulative effect of these features is that the phase boundaries, indicated by the points of tangency, are nearly the same for CMC and DL0. The right-side point of tangency is at slightly higher concentration for DL0 than for CMC, due to the slightly steeper slope of the DL0A curve. This causes the DL0 tangent to be slightly steeper than the CMC tangent. Consequently, the left-side point of tangency on the DL0I curve is at very slightly lower concentration than that on

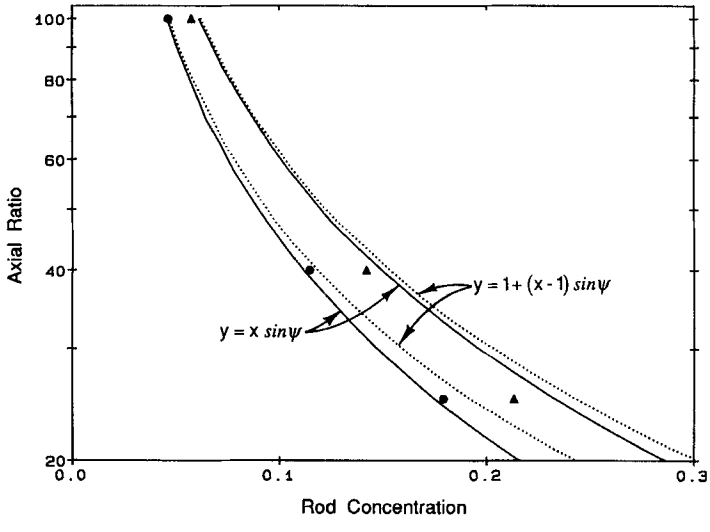

FIGURE 6 Portion of phase diagram for two-dimensional system with uniform orientation distributions imposed. Lines are for the DLM with the alternate expressions for y, as indicated. Points are generated by the CMC method.

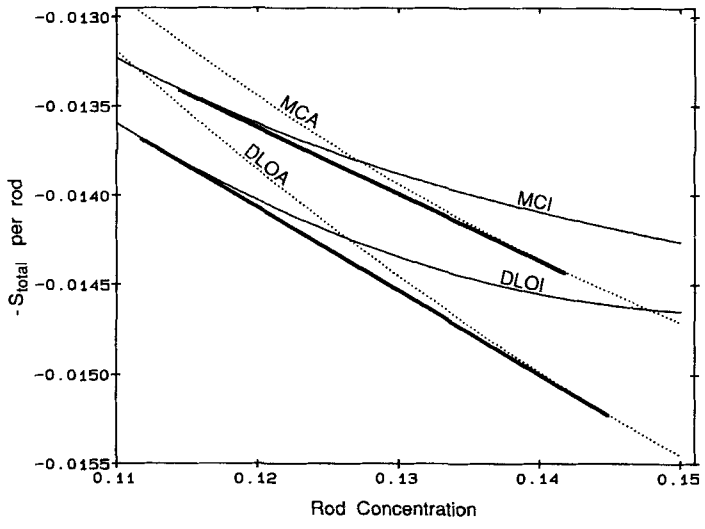

FIGURE 7 Detail of free energy curves from Figure 5. Only CMC (MCA and MCI) and DLM with $y = x \sin \psi$ (DL0A and DL0I) are shown. The respective common tangents are also included (bold lines).

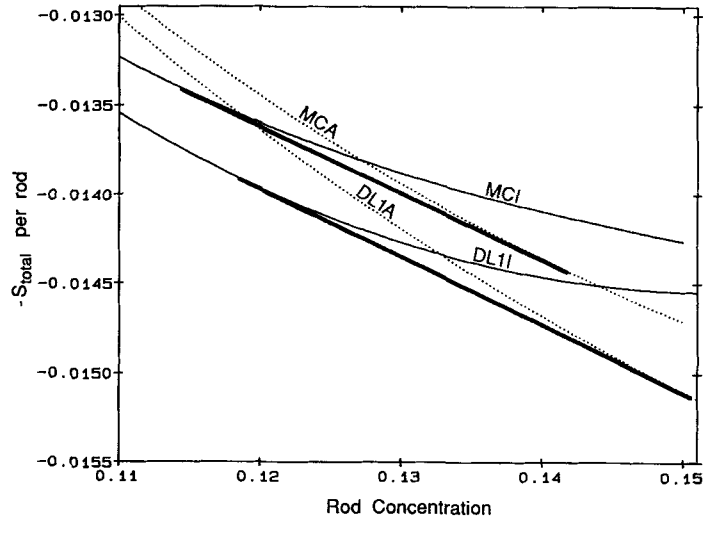

FIGURE 8 Same as Figure 7 except that the DLM curves are those for $y = 1 + (x - 1)\sin \psi$, (DL1A and DL1I).

the CMC curve. These relationships also occur at the other axial ratios tested by CMC, as indicated by Figure 6 (compare the CMC results to the solid lines).

Now consider the comparison of the CMC with the DL1 curves in Figure 8:

a) The anisotropic phase curves, MCA and DL1A, are more closely spaced than the isotropic phase curves, MCI and DL1I.

b) MCI and DL1I are nearly parallel on the left side.

c) DL1A slopes slightly more than MCA.

In this case, both points of tangency, left and right, are at higher concentrations for DL1 than for CMC, with the difference on the right pair being the largest. This change, which is again reflected in Figure 6 (compare the CMC results to the dotted curves), is due mainly to the fact that the spacing between the anisotropic phase curves is smaller than that between the isotropic phase curves, unlike the relationship seen in Figure 7. The change is caused by use of $y = 1 + (x - 1)\sin\psi$—the alternative expression for number of segments—for calculation of DL1, rather than $y = x \sin\psi$, which was used in calculating DL0. As discussed above, the alternative expression for y brings the DLM closer to a true representation of rods at low disorientation; rods that are perfectly aligned with the domain axis are assigned one, rather than zero segments. The alternative expression has a greater effect on the calculated fraction-of-vacancies in the anisotropic phase than in the isotropic phase. Recall that for our two-dimensional model, the fraction-of-vacancies expression for the isotropic phase retains dependence on y, because $\hat{y}$ is not equal to x in the two-dimensional isotropic case. Nevertheless, the isotropic phase is affected only slightly; most of the difference between DL0 and DL1 is seen in the anisotropic phase and this is what causes the anisotropic phase curves to be more closely spaced than the isotropic phase curves in Figure 8.

Because the angular distributions analyzed by the three methods were identical (uniform, $\langle\psi\rangle = 15°$), and the orientational entropy calculations were also identical, the differences between the sets of free energy curves are due solely to differences in calculated combinatoric entropy. If we are willing to accept two premises,

a) that use of the alternative expression for y in the DLM gives a more accurate representation of the degree of disorder in a configuration of rods, and

b) that the CMC results, based on measurements of realistic rod configurations, give the true vacancy fractions,

then we can regard the difference between the results in Figure 8, for DL1 versus CMC, as a reflection of the DLM's innate properties. That is, we can consider the difference between CMC and DL1 as being due mainly to the difference in estimation of vacancies rather than being due to problems with estimation of both the number of segments and the vacancy fractions. Accepting these premises, we can say that the DLM tends to overestimate the fraction-of-vacancies in the isotropic phase to a greater extent than it overestimates the fraction-of-vacancies in anisotropic phases. In a sense, the DLM favors disorder. Both phases are assigned lower free energy than they are by the CMC technique, but more so for the isotropic phase. This relative bias in favor of the isotropic phase has the effect of displacing the phase boundaries to higher concentrations, as seen in Figure 6.

The method of finding the disorder of the first anisotropic phase to appear, discussed in connection with Figure 7 of the preceding paper,[1] works well for numerical calculations with the DLM since these calculations can be made as precise (not necessarily as accurate) as desired. However, due to the characteristic flatness of the minimum in the lower biphasic boundary curve it is very difficult to perform the similar procedure as precisely using CMC. The results of 15 CMC runs for $x = 100$, shown in Figure 9, indicate that the first anisotropic phase to appear at that axial ratio has $\langle\psi\rangle$ somewhere between 14° and 20°, probably closer to 20°. Proper adjustment of $\langle\psi\rangle$, to higher values for the CMC results would cause move-

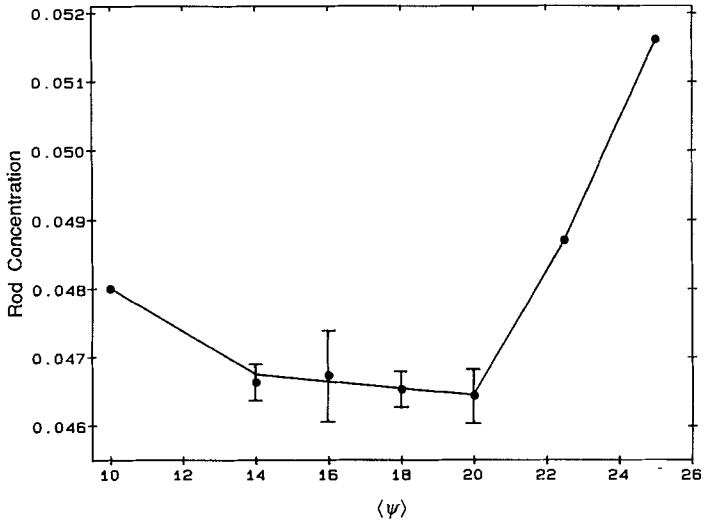

FIGURE 9 CMC-generated data for $x = 100$. The data are predictions for the concentration at the lower biphasic boundary as a function of the order parameter, $\langle\psi\rangle$. The minimum indicates $\langle\psi\rangle$ for the phase with uniform orientation distribution in equilibrium with the isotropic phase in the two-phase region. Points with error bars ($\langle\psi\rangle = 14°$ to 20°) are the mean of three separate CMC runs. Other points are for single CMC runs.

ment of the upper biphasic boundary to lower concentrations, but would affect the lower biphasic boundary imperceptibly. Thus, we suspect that the true difference between the CMC and DL1 upper biphasic boundaries is slightly greater than that indicated in Figure 6.

Phase Equilibria for Normally Distributed Orientations

DLM predicts continuous phase transitions in two dimensions for the systems with normally distributed orientations, just as does the CMC.[1] Attempts to find the critical disorder index, indicating phase separation, do not produce a minimum in the lower biphasic boundary, as was discussed in the preceding paper.[1] The results suggest a smooth evolution of increasing order as the rod concentration is increased.

CMC results for normally distributed orientations[1] are plotted with those for the DLM in Figure 10. Contours of σ values are indicated by finding where the free energy curves for two phases with normally distributed orientations with different σ cross. (The contours then indicate the concentrations where the distribution is expected to have a σ intermediate to those used in the crossing calculation.) We can see that CMC agrees closely with DL1 for the concentrations where $\sigma = 80°$ crosses $\sigma = 40°$. However the 40°/20° contours for both versions of the DLM are at significantly higher concentrations than that for CMC.

The same principles that were discussed previously in relation to uniform orientation distributions apply to the behavior of normally distributed orientations, even though phase separation is not detected. The DL1 results (dotted lines in Figure 10) again reflect overestimation of the fraction-of-vacancies in highly disordered phases—relative to phases with less disorder—when the CMC results are

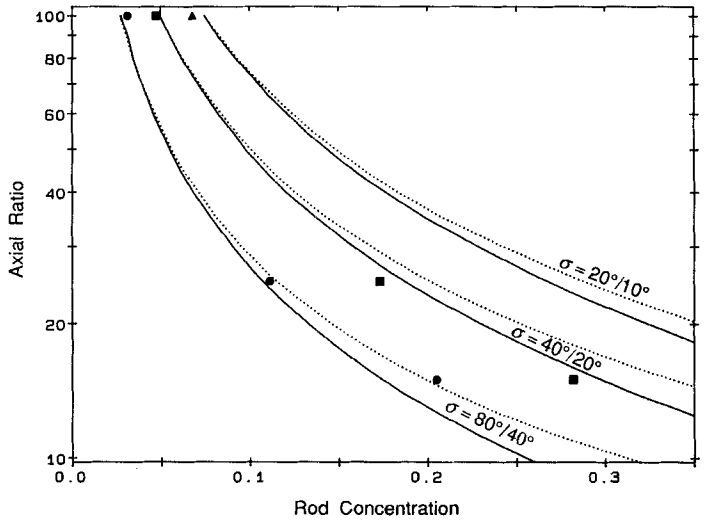

FIGURE 10 Portion of phase diagram for two-dimensional system with normally distributed orientations imposed. Contours are predictions of crossing points for the respective free energy curves, indicating continuously changing order parameter in the system. Lines are for the DLM with $y = 1 + (x - 1)\sin\psi$ (dotted) or $y = x \sin\psi$ (solid). Points are generated by the CMC method.

used as the standard. Again, the DLM favors disorder. CMC matches closely with DL0 at the 80°/40° contour because there is not much difference in the vacancy fractions for configurations with these distribution widths; both are significantly truncated at $\psi = \pi/2$, and both have relatively high degrees of disorder, approaching that of the isotropic phase. On the other hand, there is a significant difference in vacancy fractions between $\sigma = 20°$ and $\sigma = 40°$, allowing the high-disorder bias of the DLM to take effect. This explains the results in Figure 10, where CMC and DL1 agree closely for the 80°/40° contour, but not for 40°/20°.

Comparison of Distribution Shapes

We have so far discussed results for two global orientation distribution shapes, the uniform orientation distribution, which produces a first order phase transition in the two dimensional system, and normally distributed orientations, which produce a continuous phase transition. In this section, we examine the ability of the DLM to distinguish the "correct" orientation distribution shape, given the choice between several shapes, all with long-range order. As discussed in the preceding paper,[1] it is widely believed that real two-dimensional systems do not exhibit true long-range order. However, we are interested here in testing the predictive ability of the DLM, not with establishing the true behavior of two-dimensional systems.

Although orientation distributions are commonly compared on the basis of order parameter[3,7,15-17] it is most logical, in the context of this discussion, to make comparisons on the basis of equal orientational entropy. As can be seen in Equation (1) of the preceding paper,[1] S_o is a linear function of the rod concentration. Since $-S_o$ is one of two components of the free energy, then the relative free energies of two distribution shapes having equal S_o will be determined solely by $-S_c$. That

is, if distributions A and B have identical $-S_o$ but A has lower $-S_c$, then we know that A has lower total free energy than B; a configuration with distribution B would spontaneously transform into A (assuming that A has the lowest free energy of any possible distribution).

Five differently shaped two-dimensional distributions, all with $-S_o = 0.8$, are shown in Figure 11. We are familiar with the normal and the uniform types. The "triangle" type is simply a straight line. The cosine squared distribution was pro-

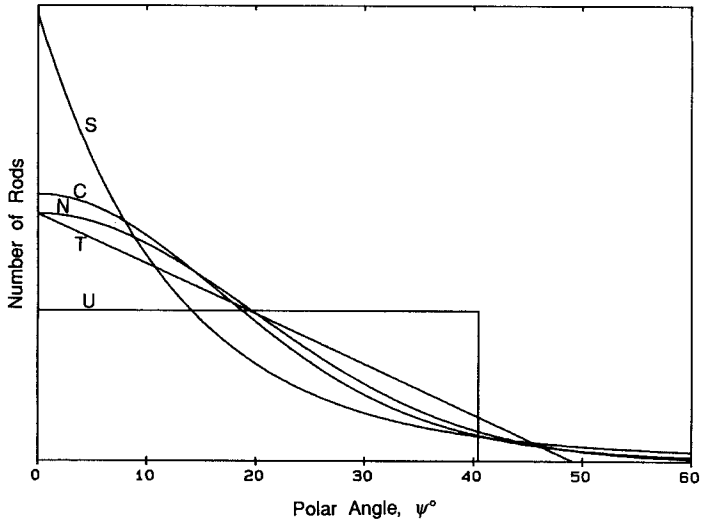

FIGURE 11 Five distribution shapes for two-dimensional configurations. All have $-S_o = 0.8$. S)sine function, C) cosine squared, N) normal, T) triangle, and U) uniform.

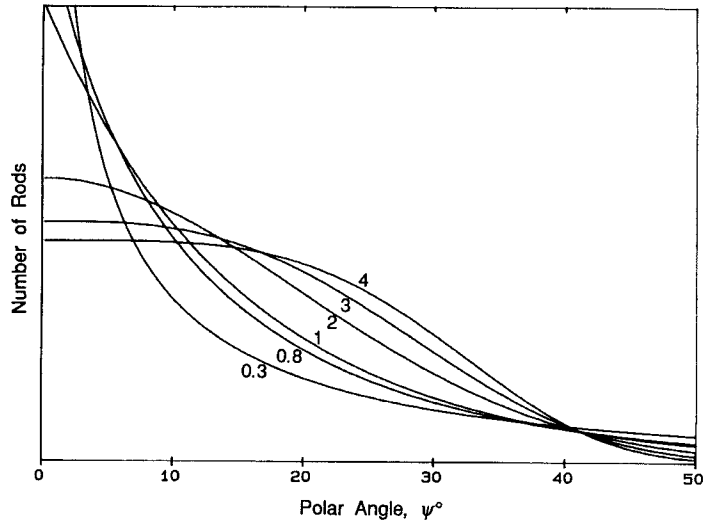

FIGURE 12 The family of distribution shapes obtained by variation of the exponential factor, XP, in Equation (22). Here σ has been adjusted so that all of these two-dimensional distributions have $-S_o = 0.8$. The curves are labeled with their exponential factors.

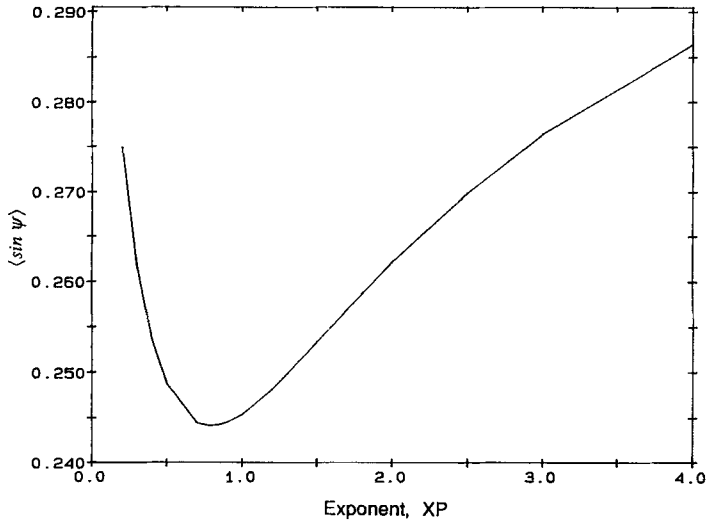

FIGURE 13 The parameter, $\langle \sin \psi \rangle$, as a function of the exponential shape factor, XP, for the family of distribution shapes shown in Figure 12. The minimum occurs at $XP = 0.8$.

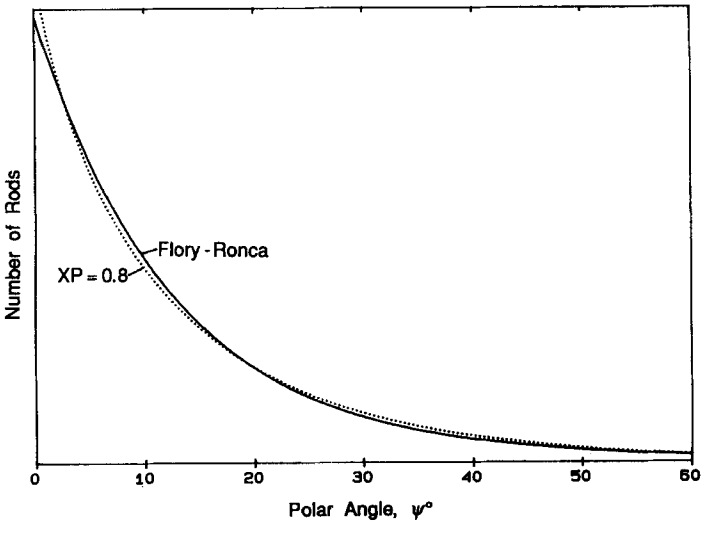

FIGURE 14 Comparison of the two-dimensional version of the Flory-Ronca distribution, Equation (21), to the exponential with $XP = 0.8$, Equation (22).

posed by Alben[17] and by Lee and Meyer[18] for the three-dimensional system, and is given by:

$$m_\psi \propto \exp(P \cos^2\psi) \tag{20}$$

where P is the adjustable parameter. The sine function is the two-dimensional version of that suggested by Straley[5] and used by Flory and Ronca[3]:

$$m_\psi \propto \exp(-P \sin \psi) \tag{21}$$

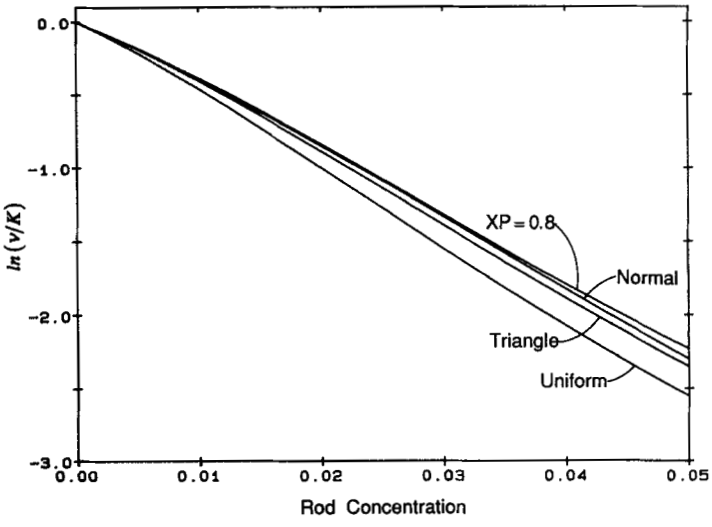

FIGURE 15 Measurements of vacancy fractions by the CMC method for four distribution shapes adjusted to $-S_o = 0.8$. Axial ratio is 100. Lines shown are polynomials fit to the Monte Carlo data.

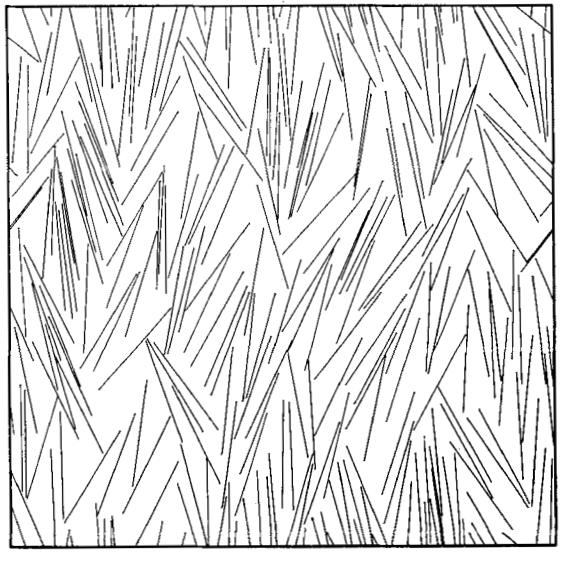

FIGURE 16 Plot of configuration built up by CMC using the exponential distribution with $XP = 4$ and adjusted to $-S_o = 0.8$. Area fraction is 0.0952, axial ratio is 100.

The fact that the combinatoric entropy in the Flory-Ronca model is determined solely by $\langle \sin \psi \rangle$, through $\hat{y}$ (as well as the rod concentration), gives us the opportunity to investigate the optimum distribution shape, as predicted by the DLM. We do this using an exponential distribution for two-dimensional systems that includes two adjustable parameters:

$$m_\psi \propto \exp(-(\psi/\sigma)^{XP}/2) \tag{22}$$

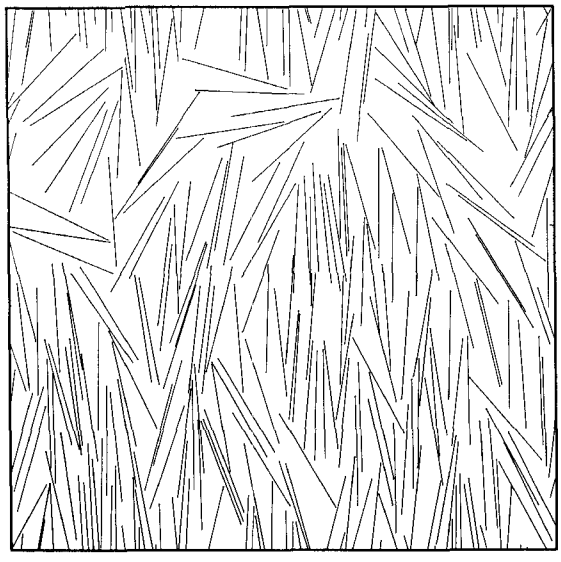

FIGURE 17 Plot of configuration built up by CMC using the exponential distribution with $XP = 0.8$ and adjusted to $-S_o = 0.8$. Area fraction is 0.0952, axial ratio is 100.

where the exponent, XP, is the shape-controlling parameter and σ is the usual width-determining factor. When $XP = 2$, we have the familiar normal distribution. A range of shapes is shown in Figure 12, each curve labeled with its shape-determining exponent, XP. All of these distributions have been adjusted in width to yield $-S_o = 0.8$, yet they give different values for $\langle \sin \psi \rangle$, as shown in Figure 13. The minimum in the curve is at $XP = 0.8$. (Equality of XP and $-S_o$ is merely coincidental, the trends happen to cross at 0.8.) Because all of the differently shaped distributions in Figure 13 have been adjusted to have identical orientational entropy, the fact that the particular distribution with $XP = 0.8$ has the lowest $\langle \sin \psi \rangle$ value—giving the lowest negative combinatoric entropy by the Flory-Ronca model—indicates that this distribution is predicted to be the most stable (by that model), with the lowest total free energy amongst those in the family of shapes given by (22). Since this prediction is based on the value of $\langle \sin \psi \rangle$, it is probably not fortuitous that this exponential has nearly identical shape to the Flory-Ronca distribution (21). The pair are shown together in Figure 14. It is apparent that Flory and Ronca chose the distribution shape (suggested by Straley) that gives the lowest total free energy when applied through their model.

We can now use the CMC technique to give an indication of whether the DLM predicts the proper distribution shape. Tests were performed on four different shapes, uniform, normal, triangle, and the exponential with $XP = 0.8$. All have $-S_o = 0.8$. The results, shown in Figure 15, indicate that the Flory-Ronca DLM and the CMC technique are in qualitative agreement for ranking this set of shapes. The exponential with $XP = 0.8$ gives the highest fraction-of-vacancies, indicating it will also give the lowest total free energy.

We must emphasize that there may be other distribution shapes that attain even lower free energy and that this analysis, which assumes long-range order, may not

be relevant to real two-dimensional systems. Nevertheless, we have obtained an indication that the DLM, despite other problems, is a relatively reliable predictor of orientation distribution shape in the anisotropic phase of monodisperse systems. This observation may also apply to use of the DLM for assessing the nature of short-range order as well.

The plots made from CMC runs and shown in Figures 16 and 17 give a physical picture of two global distributions that exhibit differences in short-range order; the "correct" distribution, Figure 17 with $XP = 0.8$, contains many more high deviation rods in its "tail" than does the distribution in Figure 16, which is an exponential with $XP = 4$ and a very much smaller tail. The distinctions between clusters of rods with similar orientation are more evident in Figure 17. Short-range order and its effects are discussed further in the following paper.[4]

CONCLUSIONS

In conclusion, conversion of the DLM to two dimensions served to clarify the role of the number-of-segments expression in Flory and Ronca's model: it insures that the calculated number of vacancies for a rod in the isotropic phase is dependent only upon the rod concentration and the axial ratio, not on the orientation of the particular rod. This motivation for the $4/\pi$ factor in Equation (11) was not clearly specified in Flory and Ronca's paper.

It was also shown that, as with the results generated by CMC,[1] choice of the shape of the global orientation distribution can result in shifting from a first order to a continuous phase transition in DLM calculations on two-dimensional systems. The DLM was found to be a reliable predictor of equilibrium orientation distribution shape for monodisperse systems.

Further, by comparison of free energy curves and phase diagrams generated by CMC and DLM, it was established that use of the DLM leads to two types of errors in calculation of relative entropies: First, short rods are assigned relatively higher entropies than are long rods, a problem that increases with increasing rod concentration. Second, in the determination of phase equilibria for monodisperse systems, phases with high degrees of disorder are "favored" over phases with low degrees of disorder.

Acknowledgment

The authors wish to thank Pacific Northwest Laboratory, ACS-PRF (no. 21300-G7) and the I.B.M. corporation for financial support and Mr. P. McGrail for computer programming advice.

References

1. L. A. Chick and C. Viney, *Mol. Cryst. Liq. Cryst.*, **226**, 25 (1993).
2. P. J. Flory, *Proc. Roy. Soc. London A*, **234**, 73 (1956).
3. P. J. Flory and G. Ronca, *Mol. Cryst. Liq. Cryst.*, **54**, 289 (1979).
4. L. A. Chick and C. Viney, *Mol. Cryst. Liq. Cryst.*, **226**, 63 (1993).

5. J. P. Straley, *Mol. Cryst. Liq. Cryst.*, **22**, 333 (1973).
6. M. Warner, *Mol. Cryst. Liq. Cryst.*, **80**, 67 (1982).
7. W. R. Romanko and S. H. Carr, *Macromolecules*, **21**, 2243 (1988).
8. L. A. Chick, *Ph.D. Dissertation*, University of Washington (1990). (Available through University Microfilms, 300 North Zeeb Road, Ann Arbor, Michigan 48106.)
9. P. J. Flory and A. Abe, *Macromolecules*, **11**(6), 1119 (1978).
10. A. Abe and P. J. Flory, *Macromolecules*, **11**(6), 1122 (1978).
11. P. J. Flory and R. S. Frost, *Macromolecules*, **11**(6), 1126 (1978).
12. R. S. Frost and P. J. Flory, *Macromolecules*, **11**(6), 1134 (1978).
13. J. Moscicki and G. Williams, *Polymer*, **23**, 558 (1982).
14. R. S. Frost, *Macromolecules*, **21**(6), 1854 (1988).
15. P. G. de Gennes, *The Physics of Liquid Crystals*, Clarendon, Oxford (1974).
16. M. Warner, *Mol. Cryst. Liq. Cryst.*, **80**, 79 (1982).
17. R. Alben, *Mol. Cryst. Liq. Cryst.*, **13**, 193 (1971).
18. S. D. Lee and R. B. Meyer, *J. Chem. Phys.*, **84**(6), 3443 (1986).